Proteomic analysis of ubiquitination-associated proteins in a cisplatin-resistant human lung adenocarcinoma cell line

XIA QIN[1], SHIZHI CHEN[2], ZONGYIN QIU[3], YUAN ZHANG[1] and FENG QIU[1]

[1]The First Affiliated Hospital of Chongqing Medical University, Chongqing; [2]The Second Affiliated Hospital of Chongqing Medical University, Chongqing; [3]College of Pharmacy, Chongqing Medical University, Chongqing, P.R. China

Received October 24, 2011; Accepted December 8, 2011

DOI: 10.3892/ijmm.2012.912

Abstract. The objective of this study was to screen for ubiquitination-associated proteins involved in cisplatin resistance in a human lung adenocarcinoma cell strain using a comparative proteomic strategy. We employed 1D SDS-PAGE to separate ubiquitinated proteins isolated and enriched from A549 and A549/CDDP lysates via affinity chromatography. The differentially expressed bands between 45-85 kDa were subsequently hydrolyzed by trypsin and subjected to HPLC-CHIP-MS/MS analysis. Of the 11 proteins identified, 7 proteins were monoubiquitinated or polyubiquitinated substrates and 4 proteins were E3 ubiquitin ligase-associated proteins. The results of western blotting and confocal laser scanning microscopy indicated that the expression levels of the E3 ubiquitin ligases RNF6, LRSAM1 and TRIM25 in A549 cells were significantly lower than those in the A549/CDDP cell line. The expression levels of the above three ubiquitin ligases in both cell lines were significantly decreased upon treatment with cis-diamminedichloroplatinum (CDDP), and the expression in the A549/CDDP cell after the treatment with CDDP decreased to a lesser extent. The expression of the substrate PKM2 in the A549 cell was higher than that in the A549/CDDP cells. Moreover, the expression of PKM2 increased in the A549 cell line and decreased in the A549/CDDP cell line upon CDDP treatment. This study suggests that drug resistance is closely correlated with changes in the ubiquitination process at the protein level in a human lung adenocarcinoma cell line.

Correspondence to: Dr Feng Qiu, The First Affiliated Hospital of Chongqing Medical University, Chongqing 400016, P.R. China
E-mail: qiufeng.cn@gmail.com

Abbreviations: CDDP, cis-diamminedichioroplatinum; UPP, ubiquitin-proteasome pathway; MTT, 3-(4,5-dimethylthiazol-2-yl)-2,5-diphenyltetrazolium bromide; DMSO, dimethyl sulfoxide; MG132, Z-Leu-Leu-Leu-al; UBD, ubiquitin binding domain

Key words: ubiquitinated proteome, ubiquitination, cisplatin resistance, drug resistance, lung adenocarcinoma cell line

Introduction

cis-Diamminedichloroplatinum (cisplatin CDDP) is one of the most commonly used drugs for the chemotherapy of lung cancer. However, the chemotherapy does not always lead to optimal effects and can even lead to treatment failure due to cisplatin resistance in tumor cells. In this regard, exploring the molecular mechanism and countermeasures of cisplatin resistance remains a hot spot in cancer research. *In vivo* and *in vitro* studies have hitherto found that tumor drug resistance is associated with mutation and amplification of target genes, variations in the capacity of repairing DNA damage and decreased concentrations of drugs in tumor cells, suggesting the complexity of the molecular mechanism of drug resistance and the necessity of further investigation using genomics, proteomics, epigenetics, and bioinformatics (1-3).

Ubiquitination, the most crucial form of protein modification in eukaryotic cells, plays vital physiological roles, including eliminating aberrant proteins and regulating the cell cycle, DNA repair, the growth of cells and immune functions (4-7). It is also documented that ubiquitin exhibits an array of non-proteolytic activities, such as involvement in vesicular transport pathways, regulation of histone modifications and activation of protein kinases and phosphatases (8).

Some studies have noted the connections between ubiquitination and the ubiquitin-proteasome pathway (UPP) and the molecular mechanism of drug resistance of tumor cells. For example, the stability and function of the important multidrug resistance-associated protein P-glycoprotein (P-gp) are regulated by UPP and thus change the drug sensitivity of multi-drug resistance cells (9). The expressed products of the proto-oncogene c-jun degraded by UPP can regulate the activity of the transcriptional factor AP-1, and the increased activity of AP-1 is related to drug resistance in the cisplatin-resistant ovarian cancer cells (10). The results of these studies indicate that investigating the relationships between ubiquitination and the drug resistance of tumor cells is of great significance.

On the basis of investigations of the human lung adenocarcinoma cell strain A549 and the cisplatin-resistant cell strain A549/CDDP, we screened for differentially expressed proteins related to ubiquitination in the cisplatin-resistant cell strain by using 1D SDS-PAGE and HPLC-CHIP-MS-MS from ubiquitinated proteins enriched by affinity chromatography,

and we validated the results by western blotting and confocal laser scanning microscopy. We aimed to provide novel experimental evidence at the proteomic level for the exploration of the changes in UPP in cisplatin-resistant lung cancer cells.

Materials and methods

Cell culture. The human lung adenocarcinoma cell strain A549 and the cisplatin-resistant human lung adenocarcinoma cell strain A549/CDDP were purchased from the Shanghai Rui Cong Laboratory Equipment Co., Ltd. (Shanghai, China). Cells were cultured in RPMI-1640 medium (Gibco, USA) containing 10% (v/v) fetal new born serum (NBCS; Gibco), 100 IU/ml penicillin and 100 μg/ml streptomycin at 37˚C, 50 ml/l CO_2 and saturated humidity. To maintain drug resistance, A549/CDDP cells were cultured with 2 μg/ml cisplatin (Sigma-Aldrich, St. Louis, MO, USA) and were further cultured in DDP-free RPMI-1640 medium two days before starting the experiment.

Cytotoxic assay. The cells at the exponential growth phase were seeded in 96-well plates at a density of $5x10^3$ cells/well (200 μl/well) and cultured at 37˚C with 5% CO_2 for 12 h. Then, equal volumes of 20 μmol/l CDDP and 5% glucose solution were added to the experimental group and the control group, respectively. After incubation at 37˚C and 5% CO_2 for 48 h, the supernatant was decanted, and each well was supplemented with 20 μl of 5 mg/ml MTT (3-(4,5-dimethylthiazol-2-yl)-2,5-diphenyltetrazolium bromide) (Sigma-Aldrich). After incubation for 4 h, the supernatant in each well was removed, and 150 μl of DMSO (dimethyl sulfoxide) was added. The 96-well plates were shaken at room temperature to dissolve the precipitates. Optical density (OD) at 570 nm was recorded on a microculture plate reader 400ATC (SLT Labinstruments, Austria). The half maximal inhibitory concentration (IC_{50}) was measured by linear regression. Resistance index (RI) = IC_{50}(A549/CDDP)/IC_{50}(A549).

Cell proliferation assay. Cells at the exponential growth phase were seeded in 96-well plates at a density of $2x10^3$ cells/well (200 μl/well) and cultured at 37˚C with 5% CO_2 for 12 h, followed by the addition of 20 μmol/l CDDP and incubation at 37˚C and 5% CO_2. The cell proliferation was determined by MTT within 5 days.

Images of living cells. A549 cells and A549/CDDP cells were separately seeded in two 6-well plates ($3x10^5$ cells/well). The 12 h culture was supplemented with 20 μmol/l CDDP and incubated for 48 h. The cellular morphology was observed under a DMI IL/3000B inverted microscope (LEICA, Nussloch, Germany) and a JEM-1200 transmission electron microscope (JEOL, Tokyo, Japan).

Transmission electron microscopy. After digestion with trypsin for 5 min and washing with PBS twice, the cells were harvested by centrifugation (1500 r/min for 15 min) and fixed with the addition of 2.5% ice-cold glutaraldehyde (pH 7.2) at 4˚C for 2 h. Subsequently, the cells were washed with ice-cold PBS at 4˚C and subjected to secondary fixation with 1% osmium tetroxide at room temperature for 2 h. The cells were further dehydrated with an ethanol gradient and acetone (2x15 min). Cells embedded in Epon-812 resin were sectioned by an LKB ultramicrotome (Ultrotome NOVA; LKB, Broma, Sweden) and stained by uranyl acetate and lead citrate. The cellular morphology was observed and photographed on a JEM-1200 transmission electron microscope.

Flow cytometry. Apoptosis was detected by Annexin V-FITC/PI double-labeled cytometry by using the Annexin V-FITC apoptosis detection kit. After treatment with CDDP for 48 h, cells were washed with PBS and harvested. The cells were resuspended in 500 μl of binding buffer (1-$5x10^5$ cells) with 5 μl of FITC (Annexin V-fluorescein isothiocyanate) and 5 μl of PI (propidium iodide) and were incubated in the dark at room temperature. The flow cytometric analysis was performed on a FACScan flow cytometer (Becton-Dickinson, Sunnyvale, CA, USA).

PI staining was used for flow cytometric analysis of the cell cycle. After treatment with CDDP for 48 h, cells were harvested and washed twice with ice-cold PBS. The cells were fixed in 70% ice-cold ethanol at 4˚C overnight. The cells, harvested by centrifugation, were washed with PBS and incubated with 50 μg/ml PI (PBS supplemented with 20 mg/ml RNase, 50 μg/ml PI, and 0.05% Triton X-100) in the dark at 4˚C for 30 min. The cell cycle stage was detected by flow cytometry. The results were analyzed by the cell-cycle analysis software ModFit LT.

Isolation, enrichment and verification of ubiquitinated proteins. A549 cells and A549/CDDP cells were seeded in two 6-well plates ($3x10^5$ cells/well). The overnight culture was supplemented with 20 μmol/l CDDP and incubated for 48 h. CDDP was replaced by 5% glucose in the control group. The cells were then cultured overnight in DMEM (with 10 μmol/l MG132) and washed twice with PBS. A cocktail of protease inhibitors (Roche Diagnostics, Laval, Canada) and a modified RIPA lysis buffer (50 mmol/l Tris-HCl pH 7.4, 150 mmol/l NaCl, 1% NP-40, 0.25% Na-deoxycholate, 1 mmol/l EDTA) containing 10 mmol/l deubiquitination inhibitor N-ethylmaleimide were lysed by sonication (2x30 sec, incubated on ice for 30 min). The cell lysates were centrifuged at 13,000 rpm for 30 min. A Bradford assay was used to determine the protein concentrations of the supernatants. The UbiQapture™-Q kit (UW8995; ENZO LifeSciences, Lörach, Germany) was used to isolate and enrich ubiquitinated proteins. The isolated and enriched ubiquitinated proteins from three independent batches were amalgamated in EP tubes and frozen at -80˚C overnight for subsequent lyophilization. The samples were resolved in 40 μl of 5X loading buffer. The ubiquitinated proteins obtained were detected by western blotting using a ubiquitin-conjugate specific HRP-linked antibody (1:1,000 dilution).

1D SDS-PAGE separation of ubiquitinated proteins. The elution fractions (EF) from the UbiQapture™-Q kit were separated through SDS-PAGE (on a 10% separating gel and a 6% condensing gel). The SDS-PAGE was performed in the mini-Protein 3 Cell (Bio-Rad, Hercurles, CA, USA) vertical electrophoresis apparatus at 120 V for 30 min (30 μl of sample in each well). Following electrophoresis, the gel was stained with Coomassie Brilliant Blue R-250, scanned and analyzed by the Quantity One (Bio-Rad) software.

In-gel digestion. Differentially expressed protein bands on the 1D SDS-PAGE gel were excised and transferred into a 0.5 ml siliconized tube. The band pieces destained with the destaining solution [75 mmol/l NH_4HCO_3-40% ethanol, v/v (1:1)] were reduced with 5 mmol/l dithiothreitol (DTT)/25 mmol/l NH_4HCO_3 (volume sufficient to cover the gel) at 60˚C for 30 min and cooled down to room temperature. The supernatant was discarded. After alkylation with the addition of 55 mmol/l iodoacetamide and incubation for 30 min, the band pieces were dehydrated with 100% ACN and dried. The dehydrated gel was digested in 10 ml of 25 mmol/l NH_4HCO_3 buffer containing 20 mg/ml modified sequencing grade trypsin (Promega, Madison, WI) and incubated at 37˚C overnight. The trypsinized peptide mixture was eluted from the gel with 0.1% formic acid and dried.

Nano LC-MS/MS analysis. Peptide mixtures were resuspended in 25 μl 0.1% formic acid, and 20 μl was used for each LC-MS/MS analysis. An Agilent 1200 series nanoflow HPLC system (Agilent Technologies, Palo Alto, CA, USA) was run in the trapping mode with an enrichment column (560.3, 5 mm particles) and a Zorbax 300SB C18 analytical column (150 0.075 mm, 3.5 mm particles). The sample was injected on the enrichment column via an autosampler. The mobile phase consisted of solvents A (water with 0.1% formic acid) and B (90% ACN, 10% water with 0.1% formic acid). The column was developed with a biphasic gradient of solvent B from 3 to 15% in solvent A in 2 min followed by an increase of B from 15 to 50% in 70 min. The column was regenerated by 10 column volumes of 90% B followed by 5 volumes of 3% B. Both the enrichment and the analytical columns were submitted to the same development, washing and regeneration conditions. The total analysis time was 120 min, and the flow rate was fixed at 0.3 ml/min. ESI-MS and CID-MS/MS analyses were conducted on an Agilent 1100 Series LC/MSD Trap MS. The MS and MS/MS conditions employed were as follows: drying gas flow, 4 l/min, 3251 C; capillary voltage, 1,900 V; skim 1, 30 V; capillary exit, 75 V; trap drive, 85; averages, 1; ion current control, on; maximum accumulation time, 150 msec; smart target, 500,000; MS scan range, 300-2,200; ultra scan, on; MS/MS: number of parents, 5; averages, 1; fragmentation amplitude, 1.3 V; Smart Frag, on, 30-200%; active exclusion, on, 2 spectra, 1 min; prefer 12, on; exclude 11, on; MS/MS scan range, 200-2,000; ultra scan, on; ion current control target, 500,000. Due to statistical fluctuations of peptide precursor selection during MS/MS acquisition, three LC-MS/MS assays were run with each sample for proper proteome comparison.

Protein identification and data analysis. The resulting peptides and proteins were automatically identified using the Spectrum Mill MS Proteomics Workbench (Rev A.03.03.078, Agilent Technologies) software. The acquired data were processed to generate peak lists using the Spectrum Mill data extractor program. The following parameters were used: scans with the same precursor ±1.4 m/z were merged within a time frame of ±15 sec. The lowest S/N ratio of the precursor was 25; the maximal charge was 7; ^{12}C peak was detected by extracting data; the $[M+H]^+$ range was 450-4,000; scanning time was 0-300 min. Peptide identification was achieved using the Spectrum Mill MS Proteomics Workbench (Rev A.03.03.078) software for automatic searching for the sequences of trypsin-digested peptides in UniProtKB/SWISS-PROT (Geneva, Switzerland), Homo Sapiens (human) protein database. Database search parameters were as follows: the allowable errors in the precursor mass and the fragment ion mass were ±2.5 and ±0.7 Da, respectively. The maximal number of the missed cleavage sites was 2. The fixed and variable modifications were specified as carbamidomethylation cysteines and oxidized methionine, respectively. The scores of complete proteins with the lowest score 70% were greater than 13. The scored peak intensities (SPI) of individual peptides were used as auto-validation criteria, which provided a good compromise between the emergence of false positive values and the loss of real values. Loose and strict criterions for parameters could result in the emergence of false positive values and the loss of real values, respectively. All the LC-MS/MS data in this study needed to be auto-validated to ensure that the data could be analyzed equally and that the results would be comparable.

Western blotting. The cellular expressions of RNF6, TRIM25, LASAM1 and PKM2 were detected by western blotting. Fifty micrograms of proteins were extracted from A549 and A549/CDDP cells (treated with 20 μmol/l CDDP), mixed with Laemmli's loading buffer, and boiled for 5 min. The cooled samples were loaded and run on a 10% SDS-PAGE gel. Proteins on the gel were blotted onto a PVDF membrane (Millipore). After blocking with 5% skim milk (w/v) in PBS-T [10 mmol/l PBS (PH 7.4), 0.1% Tween-20] for 4 h, the PVDF membrane was incubated with blocking buffer-diluted primary antibodies anti-TRIM25, anti-RNF6, anti-LASAM1, anti-PKM2 (all from Abcam, Cambridge, UK), and the mouse anti-GAPDH antibody (Sigma-Aldrich) as control at 4˚C overnight. The membrane was washed with PBS-T (3X) and incubated with the horseradish peroxidase-conjugated (HRP) goat anti-mouse secondary antibody (diluted 1:1,000 in blocking buffer, Beijing Zhongshan-Golden Bridge Biotech Co., Ltd.) at room temperature for 2 h. The membrane was then washed and incubated with the ECL kit (Millipore, USA) to detect the antibody-bound proteins on the membrane. The Chemidoc XRS system (Bio-Rad) was employed for film exposure and development. The results were analyzed by the PDQuest 7.1 software (Bio-Rad). The Quantity One 4.5 tool (Bio-Rad) was used to measure the optical density.

Confocal laser scanning microscope. A549 and A549/CDDP cells seeded in 24-well plates and cultured adherently overnight were grown on coverslips and treated with 20 μmol/l CDDP for 48 h. Cells were washed with fresh PBS at 37˚C, fixed with 4% paraformaldehyde at room temperature for 30 min, and permeabilized with 0.5% Triton X-100 at 37˚C for 15 min. After blocking with 10% goat serum for 30 min, cells were treated with mouse anti-human primary antibodies anti-TRIM25 (Abcam, diluted 1:1,000 in blocking buffer) and anti-PKM2 (Abcam, diluted 1:1,000 in blocking buffer) and incubated at 4˚C overnight. Cells were then washed with PBS (3X) and treated with FITC-conjugated (HRP) rabbit anti-mouse secondary antibody (diluted 1:1,000 in blocking buffer, Beijing Zhongshan-Golden Bridge Biotech Co., Ltd.). After incubation in the dark at 37˚C for 90 min and washing with PBS (3X), the cells on coverslips were sealed with 50%

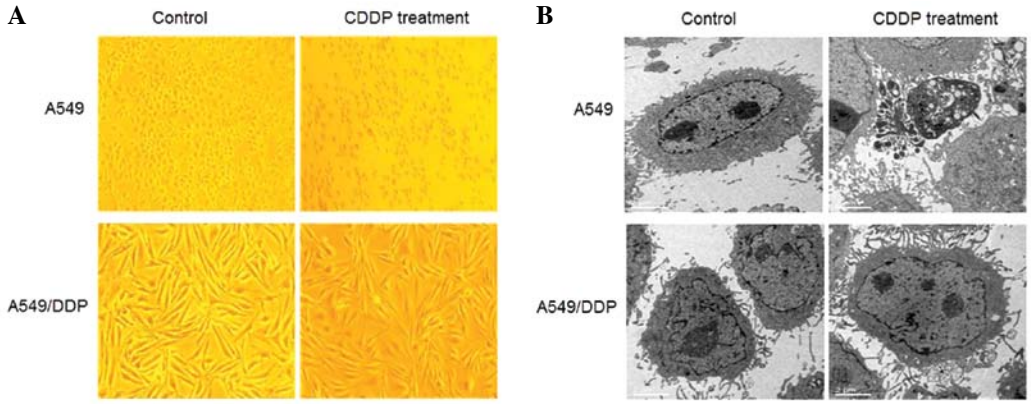

Figure 1. The morphological changes of A549 and A549/CDDP cells were untreated or treated with 20 μmol/l for 48 h by (A) inverted microscope (x100) and (B) transmission electron microscopy (x8,000). Representative images from four independent experiments are shown.

Table I. Cisplatin toxicity profile of A549 and A549/CDDP cell lines.

	IC_{50}(μmol/l)	RI
A549	8.53±0.36	-
A549/CDDP	133.35±2.12	15.63

The growth inhibition effect of cisplatin after 48 h of culture of the two cell lines is reported as IC_{50} values (concentration half-maximally reducing the growth of cancer cells ± SD). The resistance index (RI) is calculated by dividing the IC_{50} value of the resistant cell lines over that of the drug-sensitive A549 cells.

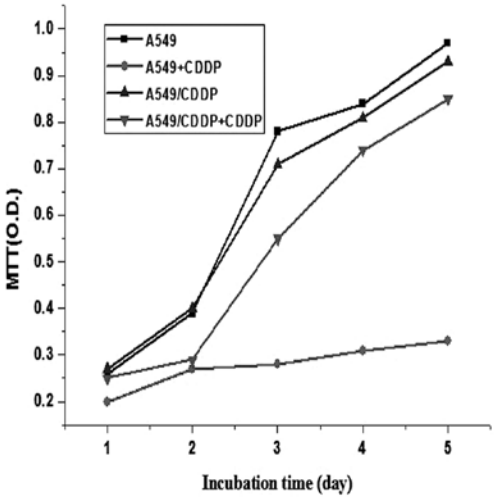

Figure 2. Cisplatin-mediated growth inhibition. A549and A549 /CDDP cells were treated with 20 μmol/l of cisplatin for the indicated time points (1, 2, 3, 4 and 5 days), direct cell number was estimated and the MTT assay was performed daily.

glycerol, observed and photographed on a confocal laser scanning microscope.

Statistical analysis. Statistical analysis was conducted using SPSS 13.0. A t-test was used to assess the statistical difference. P-values <0.05 were regarded as statistically significant.

Results

Establishment of the drug-resistant cell strain and its resistant potency. The results of optical microscopy, electron microscopy, the MTT assay, and flow cytometry indicated that the established CDDP-resistant lung adenocarcinoma cell strain A549/CDDP grew well and exhibited stable drug resistance under the conditions described herein.

By optical microscopy, A549 cells and A549/CDDP cells demonstrated significant morphological differences. A549 cells were smaller in size, polygonal in shape, and eosinophilic; they had a large nucleus near the center and little cytoplasm; they had distinct and smooth borders and clean backgrounds. A549/CDDP cells were larger in size, triangular or polygonal in shape, arranged irregularly, and eosinophilic; they had a large nucleus with clearly discernible nucleoli, little cytoplasm, rough and indiscernible borders, and black-dotted backgrounds. After treating both cell strains with 20 μmol/l CDDP for 48 h, the density of A549 cells decreased remarkably; the cells shrank and became round in shape; the cell refractive index increased; a small proportion of cells floated; the amount of cytoplasmic particles increased; and the membrane blebbed. No marked changes occurred in A549/CDDP cells (Fig. 1A).

Under the electron microscope, A549 cells had smooth outer surfaces with short microvilli, chromatin was evenly distributed and enclosed within clear nuclear membranes, the electron density was low, and the borders bulged up markedly. The surfaces of A549/CDDP cells were rough with many fingerprint-like bulges, and nuclear membranes became blurred. After the treatment with 20 μmol/l CDDP for 48 h, A549 cells exhibited typical apoptotic morphological characteristics: the cells dwindled in size, cilia on the surface disappeared, cells and mitochondria swelled, microvilli were shed, the nuclei exhibited pyknosis and were distorted and fragmented, chromatin was condensed and disassembled, the cytoplasm was vacuolated, and blebs formed. Little damage was observed in A549/CDDP cells after the CDDP treatment (Fig. 1B).

The resistance index (RI) and IC_{50} values of A549 and A549/CDDP cells against CDDP were determined through the

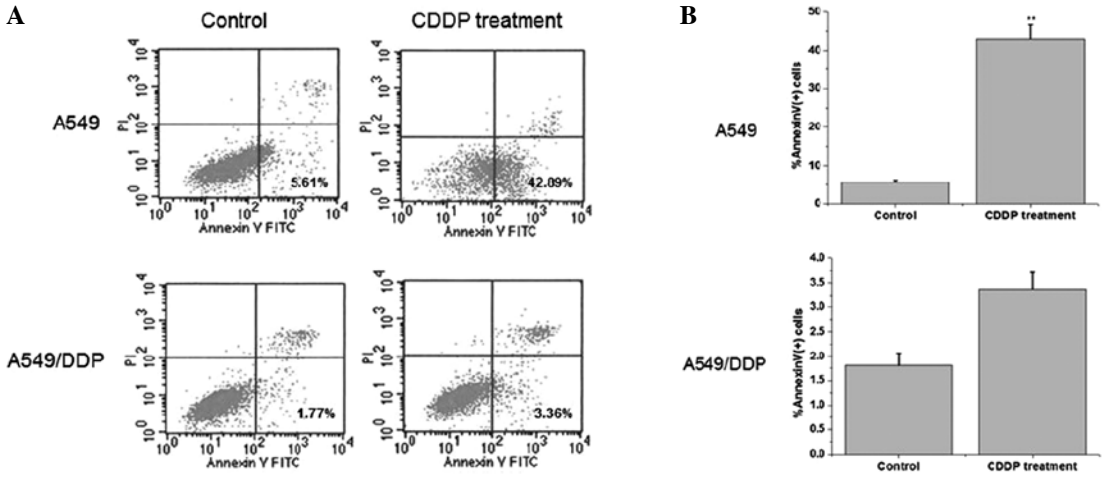

Figure 3. (A) Apoptosis of A549 and A549/CDDP cells by staining with Annexin V-FITC/PI observed by flow cytometry. (B) Apoptosis data were processed and data from three independent experiments are shown.

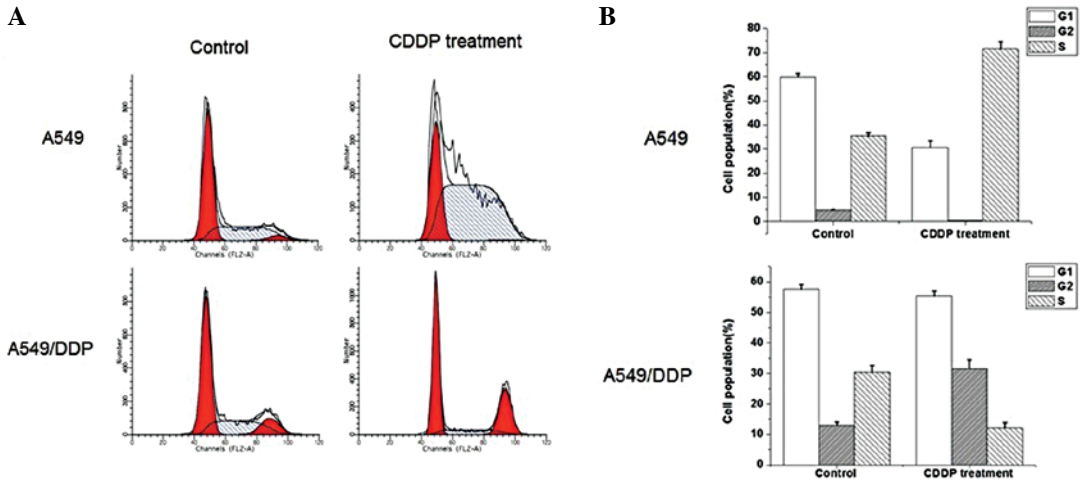

Figure 4. (A) Changes in the cell cycle distribution of A549 and A549/CDDP cells observed by flow cytometry after treatment with CDDP for 48 h. (B) Cycle distribution data were processed and data from three independent experiments are shown.

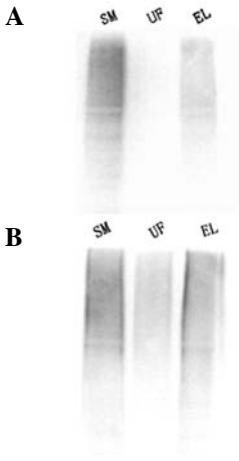

Figure 5. Western blot analysis of ubiquitin enrichment of lysate derived ubiquitinylated proteins. Ubiquitined proteins were enriched according the manufacturer's instructions and analysis of the three factions, starting material (SM), unbound fraction (UF) and elution fraction (EL) by western blot analysis using the ubiquitin-conjugate specific HRP-linked antibody provided by the kit. (A) Control ubiquitinylated-protein lysate provided by the kit. (B) One cell lysate of the sample.

MTT assay after 24 h incubation (Table I). The resistance of A549/CDDP cells to CDDP was 15 times greater than that of A549 cells, which was typical of CDDP-resistance.

The MTT assay was used to evaluate the growth of A549 and A549/CDDP cells after treatment with 20 μmol/l CDDP for 1-5 days. The inhibitory effects of CDDP on both cell strains were time-dependent. Compared with the untreated group, the growth of A549 cells was inhibited after treating with CDDP as the incubation time increased. The survival rate decreased significantly from 50% in the first day to 30% in the fifth day in comparison with the untreated group. A549/CDDP cells underwent little significant change (Fig. 2).

The results of the flow cytometry showed that after a 48 h treatment with 20 μmol/l CDDP, the apoptosis index of A549 cells was 42.97±3.65%, compared with 5.63±0.52% of the untreated group. Both the apoptosis index of A549 cells and the number of cells in the S phase increased significantly. The apoptosis indices of A549/CDDP cells before and after the treatment were 1.81±0.25 and 3.38±0.34%, respectively. No evident changes occurred, and the number of cells in the G2 phase increased markedly (Figs. 3 and 4).

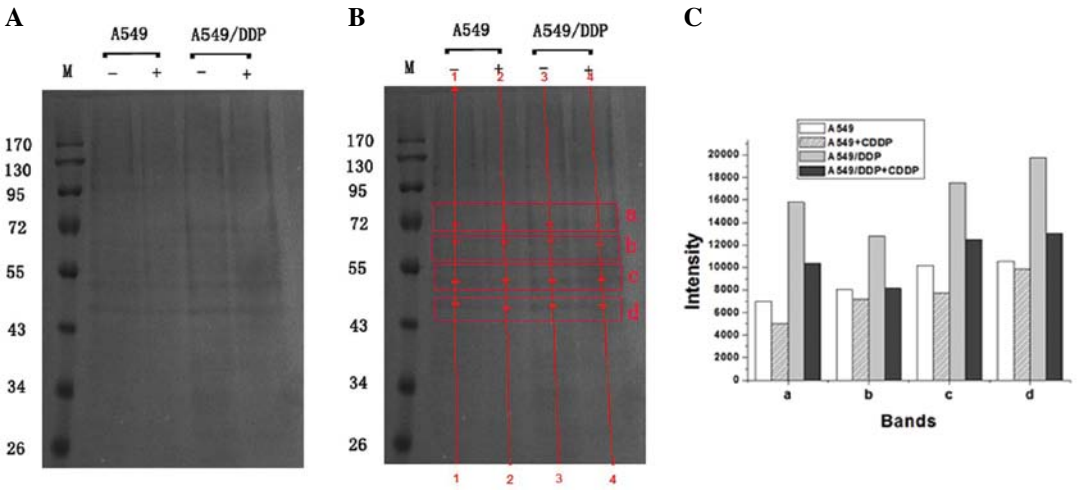

Figure 6. 1D SDS-PAGE analysis of the ubiquitined proteins captured by UbiQapture™-Q kit in A549/CDDP cells. (A) Equal volume (30 μl) of elution fractions was loaded on the gel for visualization by Coomassie blue staining. M, protein marker; -, cell line untreated with CDDP; +, cell line treated with 20 μmol/l of CDDP for 48 h. (B) Four different bands (a-d) were found through auto frame lanes and by detecting bands by the Quantity One software. (C) Intenstiy analysis of the four bands.

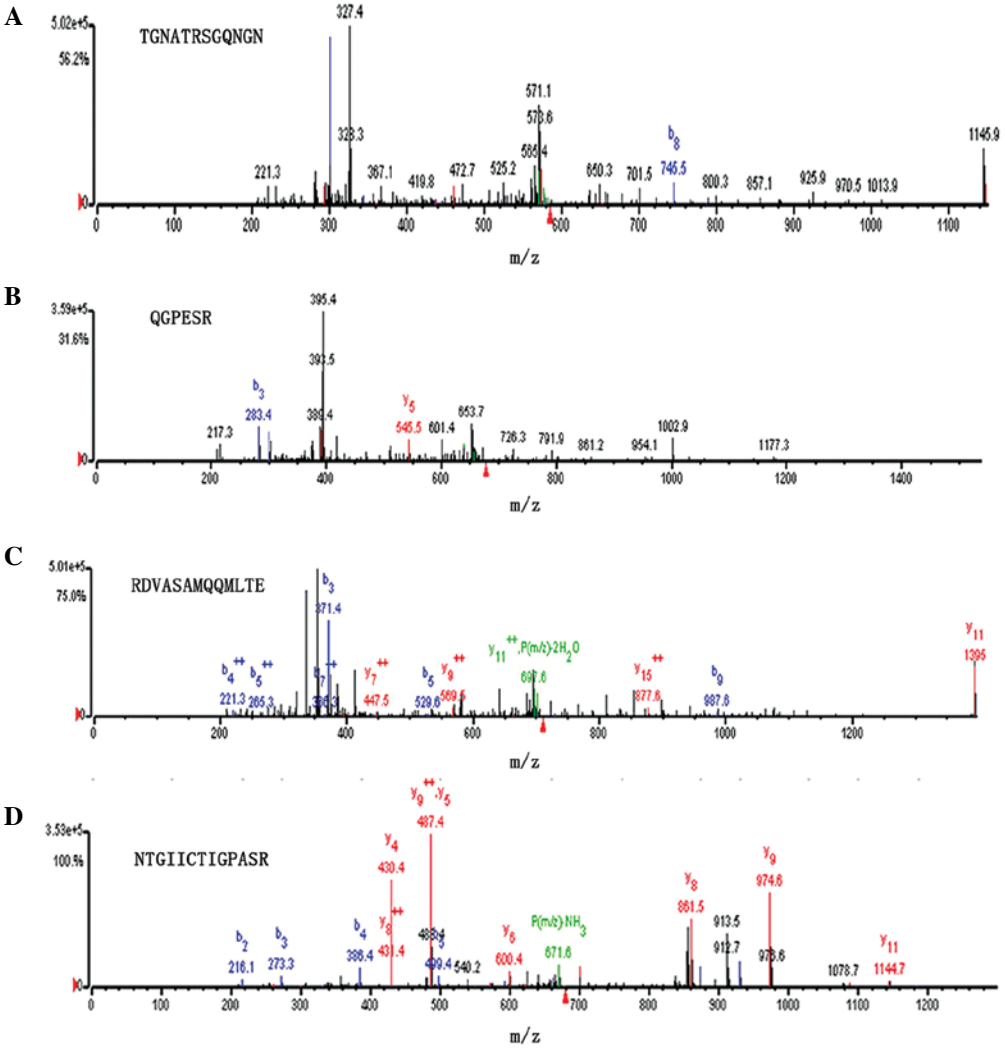

Figure 7. The MS/MS spectrum of the peptide ions from three E3 ligases and pyruvate kinase isozyme type M2. (A) MS/MS spectrum of peptide ion [TGNATRSGQNGN]$^{3+}$ (120→131, MH$^+$, 1749.5354, m/z 583.85) from RING finger protein 6. (B) MS/MS spectrum of peptide ion [QGPESR]$^+$ (536→541, MH$^+$, 675.63, m/z 675.63) from the tripartite motif-containing protein 25. (C) MS/MS spectrum of peptide ion [RDVASAMQQMLTE]$^{3+}$ (383→395, MH$^+$, 2127.0854, m/z 709.7) from leucine-rich repeat and sterile α motif-containing protein 1. (D) MS/MS spectrum of peptide ion [NTGIICTIGPASR]$^{2+}$ (44→56, MH$^+$, 1358.2127, m/z 679.61) from pyruvate kinase isozyme type M2.

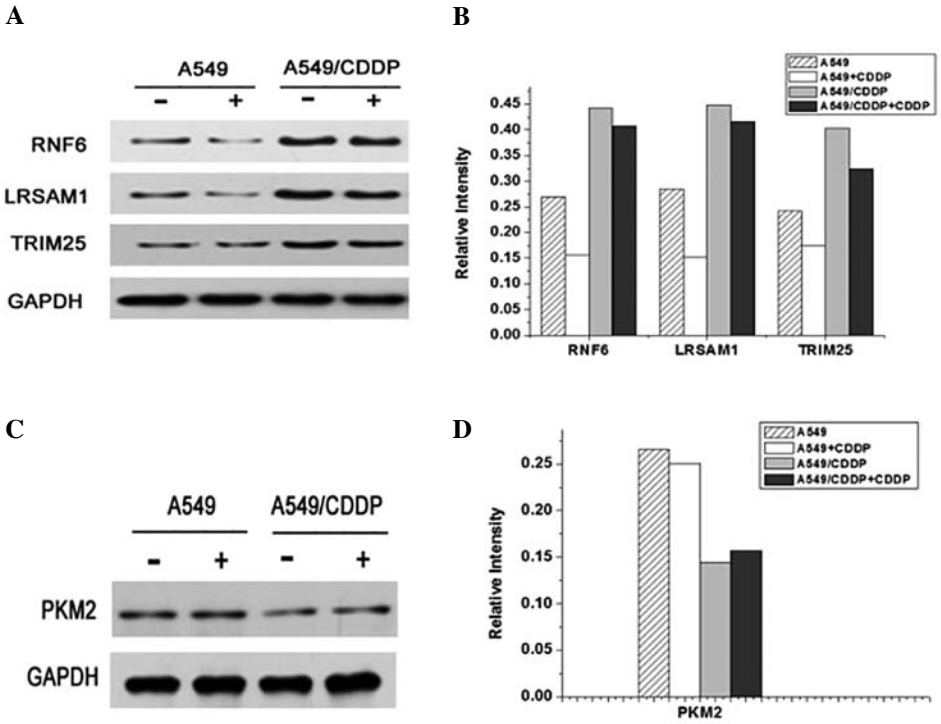

Figure 8. Western blot analysis of the expression of RNF6, TRIM25, LRSAM1 and PKM2 of control and CDDP treatment (20 μmol/l) of A549/CDDP cells. (A and C) Equal amount (50 μg) of cell lysate proteins were separated by a 10% SDS-polyacrylamide gels, transferred onto PVDF membranes and immunoblotted with antibodies against RNF6, TRIM25, LRSAM1 and PKM2. GAPDH served as a control. (B and D) The intensity analysis was performed by the Quantity One imaging software.

Isolation, enrichment, and 1D SDS-PAGE separation of ubiquitinated proteins. The western blotting assay validated that ubiquitinated proteins could be effectively isolated and enriched from A549 and A549/CDDP lysates using the high-binding affinity matrix in the UbiQapture™-Q kit (Fig. 5). The elution fraction enriched by UbiQapture™-Q via binding with the ubiquitin-binding matrix was separated by 1D SDS-PAGE and subjected to comparative image analysis. Sixteen protein bands from four regions between 45 and 85 kDa with distinct grey levels were identified and excised for the Chip HPLC-MS/MS analysis (Fig. 6).

Identification of proteins by nano-HPLC-chip-MS/MS. Ubiquitinated proteins from CDDP-treated and untreated A549 and A549/CDDP cells (between the 45 and 85 kDa bands in the 1D SDS-PAGE gel) were subjected to MS analysis. The MS/MS spectrum of the peptide ions from three E3 ligases and pyruvate kinase isozyme type M2 are shown in Fig. 7. Eleven differentially expressed proteins were identified through searching in the UniProtKB/SWISS-PROT [*Homo sapiens* (Human)] database (Table II). These included 7 potentially monoubiquitinated or polyubiquitinated proteins involved in tumor metabolism, the pentose phosphate pathway, hnRNA metabolism, mRNA splicing, Rrn3-regulated rDNA transcription, cell cycle regulation, and protein hormonal regulation. They were located in the cell nucleus, plasma, and membrane. The other 4 proteins were E3 ubiquitin ligase-associated proteins: RING finger protein 6 (RNF6), leucine rich repeat and sterile α motif containing 1 (LRSAM1), tripartite motif 25 (TRIM25), and a hypothetical protein LOC140699 isoform 3 harboring the ARM repeats domain, which was regarded as a member of the U-Box E3 ubiquitin ligase family (11). These 4 E3 ubiquitin ligase-associated proteins might be captured and identified as complexes with ubiquitinated proteins. These results indicated that the CDDP-resistant A549/CDDP cells exerted a wide-ranging influence on the ubiquitination process of proteins.

Western blotting. Western blotting yielded several interesting results. The expressions of 3 E3 ubiquitin ligase-associated proteins in A549 cells were obviously lower than those in A549/CDDP cells. They were all downregulated in A549 cells after 48 h treatment with 20 μmol/l CDDP, with an average decrease of 38.99±9.91%, while they were downregulated in A549/CDDP cells to a lesser extent with an average decrease of 13.25±9.76% (Fig. 8A and B). The expression of the substrate PKM2 in the A549 cell line was higher than that in the A549/CDDP cell line. Moreover, the expression of PKM2 was upregulated and downregulated in the A549 and A549/CDDP cells, respectively, upon 48 h of 20 μmol/l CDDP treatment (Fig. 8C and D).

LCSM analysis of TRIM25 and PKM2. The results of the confocal laser scanning microscope demonstrated that in A549 and A549/CDDP cells treated with 20 μmol/l CDDP, TRIM25 and PKM2 were primarily and evenly distributed in the plasma and were locally aggregated in the membrane. The expression of TRIM25 in A549 and A549/CDDP cells (especially in A549/CDDP cells) treated with CDDP was significantly lower than that in untreated cells (Fig. 9). The expression of PKM2 was upregulated and downregulated in the A549 cell and the A549/CDDP cell, respectively, upon

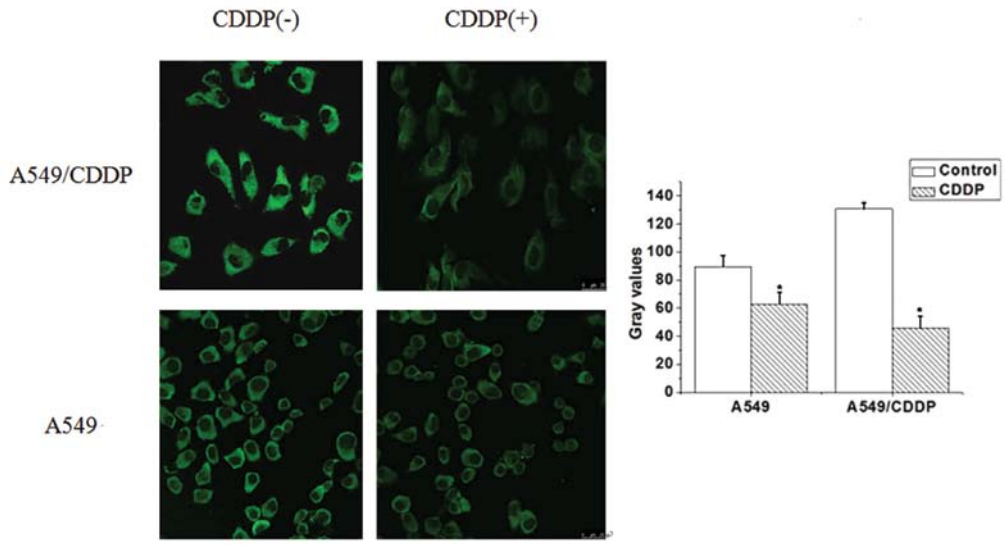

Figure 9. Differential expression level and location of TRIM25 in A549 and A549/CDDP by confocal laser scanning microscopy (FITC, x400). *P<0.01.

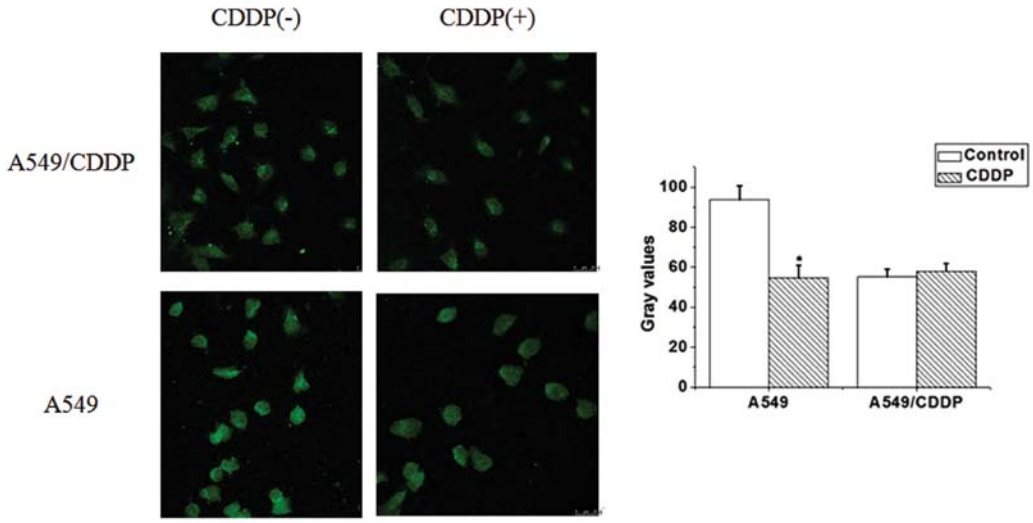

Figure 10. Differential expression level and location of PKM2 in A549 and A549/CDDP by confocal laser scanning microscopy (FITC, x400). *P<0.01.

CDDP treatment, which was consistent with the western blotting results (Fig. 10).

Discussion

Employment of a stable drug-resistant cell model is the prerequisite for relevant investigations on drug resistance of tumor cells. Low, moderate, and high levels of drug resistance are defined as RIs under 5, between 5-15, and above 15, respectively (12). Our results indicated that the RI of A549/CDDP against A549 was 15.63, and is thus a highly drug-resistant cell strain which provides a reliable cell model for this study and for further investigations.

Isolation and enrichment of ubiquitinated proteins is a critical step because of their heterogeneity and low cellular abundance. This study utilized the affinity purification technology based on ubiquitin binding domain (UBD) identification (UbiQapture™-Q kit; BIOMOL Technical Service, 2010). The UBD conjugated to the matrix was capable of identifying a variety of ubiquitination types and binding with ubiquitinated proteins. It was also applicable in combination with ubiquitination proteomics (13). The major challenge for affinity purification of ubiquitinated proteins is to remove the contaminating proteins (14), which is very difficult. Nevertheless, insoluble precipitates can be carefully removed by ultracentrifugation, and contamination can be reduced by shortening the time for incubation with the affinity matrix. This study has achieved an ideal enrichment (Fig. 5). The contents of ubiquitinated proteins in the eluates increased remarkably, which was validated by western blot analysis. The obtained continuous bands suggested that ubiquitin-conjugating enzymes might be isolated together with ubiquitinated proteins in the form of complexes, which was validated by the results of the following mass spectrum analysis.

Some studies have reported that the product of the retinoic acid-induced gene I polyubiquitinated via Lys-63 by the

Table II. Differentially expressed proteins identified by HPLC-chip/MS.

Protein name	UniprotKB/ Swissprot ID	Distinct peptides	Score	MW	PI	Subcellular location
Pyruvate kinase isozyme type M2, PKM2	P14618	9	54.31	58062.4	7.61	Cytoplasm, nucleus
Transketolase	P29401	2	16.68	67906.1	7.89	Not classified
Isoform 1 of heterogeneous nuclear ribonucleoprotein K	P61978	1	8.83	51028.5	5.19	Cytoplasm, nucleus
Hypothetical protein LOC140699 isoform 3	A2A2A4_HUMAN	1	7.21	68619.6	8.11	Not classified
U4/U6.U5 tri-snRNP-associated protein 2	Q53GS9	1	7.06	65380.8	9.02	Nucleus
RING finger protein 6, RNF6	Q9Y252	1	6.77	78091.6	9.16	Nucleus, cytoplasm
RNA polymerase I-specific transcription initiation factor RRN3	Q9NYV6	1	5.87	74107.7	5.4	Nucleus, nucleolus
ANKRD26-like family B member 3	Q86YR6	1	4.55	66665.5	8.4	Membrane
Leucine-rich repeat and sterile α motif-containing protein 1, LRSAM1	Q6UWE0	1	4.46	83594.4	5.7	Cytoplasm
Tripartite motif-containing protein 25, TRIM25	Q14258	1	4.45	70989.9	8.45	Cytoplasm
Inhibin β A chain precursor	P08476	1	7.26	47442.6	8.3	Secreted

TRIM25 E3 ubiquitin ligase was a key regulation mechanism in the RIG-I pathway (15). RNF6 facilitates degradation of target proteins by binding with the E2 ubiquitin-conjugating enzyme. Recent research indicated that RNF6 mediates the polyubiquitination of LIM domain kinase 1 (LIMK1) via Lys-48 and targets it for proteasomal degradation. Additionally, RNF6 promoted AR transcriptional activity by inducing androgen receptor (AR) ubiquitination (16,17). Polyubiquitin chain formation proceeds typically via isopeptide bond formation between the G76 carboxyl group of the 'n+1' ubiquitin to the ε-amino group of a lysine within the preceding ubiquitin. Seven lysines (K6, K11, K27, K29, K33, K48 and K63) are found in ubiquitin, allowing for the generation of a variety of polyubiquitin chain types, among which Lys-63 and Lys-48 are the two linking residues with the highest abundance (18,19). The K48-linked ubiquitination is recognized by the 26S proteasome and results in protein degradation. In contrast, the K63-linked ubiquitination does not induce protein degradation; instead, it regulates signaling activation involved in distinct biological functions such as receptor endocytosis, DNA damage repair, protein trafficking and signaling activation. Aberrant expressions of TRIM25 and RNF6 in A549/CDDP cells would lead to changes in the Lys-63/Lys-48-linked ratio, which could alter the topology of the ubiquitin chains and could eventually result in changes in proteasome targeting capabilities of some substrate proteins with important biological functions (such as RIG-I protein and LIMK1). In addition, LRSAM1 is an E3 ubiquitin ligase that mediates ubiquitination of the product of the tumor susceptibility gene 101 (TSG101) at multiple sites. Previous reports indicated that TSG101 was involved in the development of multi-drug resistance in gastric cancer and was downregulated by TSG101 siRNA to reverse this effect (20,21). Our study suggests that in A549/CDDP cells, changes in the expression level of LRSAM1 could initiate changes in the monoubiquitination process of the product of TSG101.

Pyruvate kinase M2 (PKM2) is one of the enzymes of vital significance in tumor metabolism and is closely correlated with tumorigenesis and multi-drug resistance of tumors, including CDDP-resistance. A previous study revealed a negative correlation between the expression level of PKM2 and the level of drug-resistance of tumors, and the expression level of PKM2 in A549/CDDP cells was lower than that in A549 cells. The sensitivity of A549 cells to CDDP decreased dramatically, and the drug-resistance increased markedly after the inhibition of PKM2 expression in A549 cells (22-24), in agreement with the results of this study.

Trypsin proteolysis of an ubiquitin-conjugated protein may be attenuated by the formation of isopeptide bonds in the ubiquitination process. The number of uncleaved sites could be increased by a two-residue remnant (glycine-glycine) derived from the C-terminus of ubiquitin is still covalently-attached to the target lysine residue via an isopeptide bond. This resulted in a missed proteolytic cleavage because trypsin proteolysis cannot occur at the modified lysines. (25). Consequently, the number of peptides of significance identified by mass spectrum analysis decrease, and the number of the identified proteins is reduced as a result. Similar influences also existed in this study. The number of peptides related to the identified 11 proteins was undercounted (Table II). However, in the HPLC-Chip-MS/MS system, the peptide mixture purified by affinity purification was

enriched by the HPLC-Chip before the mass spectrum analysis. The increased mass spectrometry signals offset the negative impacts of the decreased capabilities of mass spectrum analysis in the identification of ubiquitinated proteins. The signals of captured MS/MS spectra of E3 ligases and PKM2-relating peptides were enhanced with a great deal of b and y ion information. In this regard, the results of this study are reliable. However, it is suggested that close attention should be paid to the selection of conditions for mass spectrum analysis of the ubiquitinated proteome.

In conclusion, we found three E3 ubiquitin ligases in a human lung adenocarcinoma cisplatin-resistant cell strain, which suggests that drug resistance may be closely correlated with changes in the ubiquitination process at the protein level. However, proteomics is only the first step to analyze global protein expression and to find candidate proteins that may be involved in certain pathways. Further studies are necessary to investigate the role of individual proteins and sets of proteins in chemoresistance as well as in ubiquitination process.

Acknowledgements

This study was supported by funds from the key program of the Chongqing Municipal Health Bureau (no. 2011-1-036).

References

1. Fuertes MA, Alonso C and Pérez JM: Biochemical modulation of cisplatin mechanisms of action: enhancement of antitumor activity and circumvention of drug resistance. Chem Rev 103: 645-662, 2003.
2. Glasspool RM, Teodoridis JM and Brown R: Epigenetics as a mechanism driving polygenic clinical drug resistance. Br J Cancer 94: 1087-1092, 2006.
3. Telesco SE, Shih AJ, Jia F and Radhakrishnan R: A multiscale modeling approach to investigate molecular mechanisms of pseudokinase activation and drug resistance in the HER3/ErbB3 receptor tyrosine kinase signaling network. Mol Biosyst 7: 2066-2080, 2011.
4. Kikuchi A, Kishida S and Yamamoto H: Regulation of Wnt signaling by protein-protein interaction and post-translational modifications. Exp Mol Med 38: 1-10, 2006.
5. Sun Y: E3 ubiquitin ligases as cancer targets and biomarkers. Neoplasia 8: 645-654, 2006.
6. Kerscher O, Felberbaum R and Hochstrasser M: Modification of proteins by ubiquitin and ubiquitin-like proteins. Annu Rev Cell Dev Biol 22: 159-180, 2006.
7. Sunyer B, Diao WF and Lubec G: The role of post-translational modifications for learning and memory formation. Electrophoresis 29: 2593-2602, 2008.
8. Yang WL, Zhang X and Lin HK: Emerging role of Lys-63 ubiquitination in protein kinase and phosphatase activation and cancer development. Oncogene 29: 4493-4503, 2010.
9. Zhang ZG, Wu JY, Hait WN, *et al*: Regulation of the stability of P-glycoprotein by ubiquitination. Mol Pharmacol 66: 395-403, 2004.
10. Li QQ, Yunmbam MK, Zhong X, *et al*: Lactacystin enhances cisplatin sensitivity in resistant human ovarian cancer cell lines via inhibition of DNA repair and ERCC-1 expression. Cell Mol Biol 47: 61-72, 2001.
11. Mudgil Y, Shiu SH, Stone SL, Salt JN and Goring DR: A large complement of the predicted arabidopsis ARM repeat proteins are members of the U-Box E3 ubiquitin ligase family. Plant Physiol 134: 59-66, 2004.
12. Snow K and Judd W: Characterization of adriamycin- and amsacrine-resistant human leukaemic T cell lines. Br J Cancer 63: 17-28, 1991.
13. Hjerpe R and Rodríguez MS: Efficient approaches for characterizing ubiquitinated proteins. Biochem Soc Trans 36: 823-827, 2008.
14. Shi Y, Xu P and Qin J: Ubiquitinated proteome: ready for global? Mol Cell Proteomics 10: R110.006882, 2011.
15. Gack MU, Shin YC, Joo CH, Urano T, Liang CY, Sun LJ, Takeuchi O, Akira S, Chen ZJ, Inoue J, *et al*: TRIM25 RING-finger E3 ubiquitin ligase is essential for RIG-I-mediated antiviral activity. Nature 446: 916-920, 2007.
16. Tursun B, Schlüter A, Peters MA, Viehweger B, Ostendorff HP, Soosairajah J, Drung A, Bossenz M, Johnsen SA, Schweize M, *et al*: The ubiquitin ligase Rnf6 regulates local LIM kinase 1 levels in axonal growth cones. Genes Dev 19: 2307-2319, 2005.
17. Xu K, Shimelis H, Linn DE, Jiang R, Yang X, Sun F, Guo Z, Chen H, Li W, Chen H, *et al*: Regulation of androgen receptor transcriptional activity and specificity by RNF6-induced ubiquitination. Cancer Cell 15: 270-282, 2009.
18. Xu P and Peng JM: Characterization of polyubiquitin chain structure by middle-down mass spectrometry. Anal Chem 80: 3438-3444, 2008.
19. Dammer EB, Na CH, Xu P, Seyfried NT, Duong DM, Cheng D, Gearing M, Rees H, Lah JJ, Levey AI, *et al*: Polyubiquitin linkage profiles in three models of proteolytic stress suggest the etiology of Alzheimer disease. J Biol Chem 286: 10457-10465, 2011.
20. Amit I, Yakir L, Katz M, Zwang Y, Marmor MD, Citri A, Shtiegman K, Alroy I, Tuvia S, Reiss Y, *et al*: Tal, a Tsg101-specific E3 ubiquitin ligase, regulates receptor endocytosis and retrovirus budding. Genes Dev 18: 1737-1752, 2004.
21. Shen H, Pan Y, Han Z, Hong L, Liu N, Han S, Yao L, Xie H, Zhaxi C, Shi Y, *et al*: Reversal of multidrug resistance of gastric cancer cells by downregulation of TSG101 with TSG101siRNA. Cancer Biol Ther 3: 561-565, 2004.
22. Martinez-Balibrea E, Plasencia C, Ginés A, *et al*: A proteomic approach links decreased pyruvate kinase M2 expression to oxaliplatin resistance in patients with colorectal cancer and in human cell lines. Mol Cancer Ther 8: 771-778, 2009.
23. Cao LM and Hu CP: Comparative proteomics analysis of human lung adenocarcinoma cell A549 and A549/DDP. Zhong Lin Fang Zhi Yan Jin 37: 621-625, 2010.
24. Guo W, Zhang Y, Chen T, *et al*: Efficacy of RNAi targeting of pyruvate kinase M2 combined with cisplatin in a lung cancer model. J Cancer Res Clin Oncol 137: 65-72, 2010.
25. Peng J, Schwart D, Elias JE, *et al*: A proteomics approach to understanding protein ubiquitination. Nat Biotechnol 21: 921-926, 2003.